

[Click for updates](#)

Liquid Crystals

Publication details, including instructions for authors and subscription information:
<http://www.tandfonline.com/loi/tlct20>

Low threshold of distributed feedback lasers based on scaffolding morphologic holographic polymer dispersed liquid crystal gratings: reduced losses through Forster transfer

Lijuan Liu^{ab}, Wenbin Huang^{ab}, Zhihui Diao^{ab}, Zenghui Peng^a, Quan quan Mu^a, Yonggang Liu^a, Chengliang Yang^a, Lifa Hu^a & Li Xuan^a

^a State Key Laboratory of Applied Optics, Changchun Institute of Optics, Fine Mechanics and Physics, Chinese Academy of Sciences, Changchun, Jilin, China

^b Graduate School of the Chinese Academy of Sciences, Beijing, China

Published online: 07 Oct 2013.

To cite this article: Lijuan Liu, Wenbin Huang, Zhihui Diao, Zenghui Peng, Quan quan Mu, Yonggang Liu, Chengliang Yang, Lifa Hu & Li Xuan (2014) Low threshold of distributed feedback lasers based on scaffolding morphologic holographic polymer dispersed liquid crystal gratings: reduced losses through Forster transfer , *Liquid Crystals*, 41:2, 145-152, DOI: [10.1080/02678292.2013.845308](https://doi.org/10.1080/02678292.2013.845308)

To link to this article: <http://dx.doi.org/10.1080/02678292.2013.845308>

PLEASE SCROLL DOWN FOR ARTICLE

Taylor & Francis makes every effort to ensure the accuracy of all the information (the "Content") contained in the publications on our platform. However, Taylor & Francis, our agents, and our licensors make no representations or warranties whatsoever as to the accuracy, completeness, or suitability for any purpose of the Content. Any opinions and views expressed in this publication are the opinions and views of the authors, and are not the views of or endorsed by Taylor & Francis. The accuracy of the Content should not be relied upon and should be independently verified with primary sources of information. Taylor and Francis shall not be liable for any losses, actions, claims, proceedings, demands, costs, expenses, damages, and other liabilities whatsoever or howsoever caused arising directly or indirectly in connection with, in relation to or arising out of the use of the Content.

This article may be used for research, teaching, and private study purposes. Any substantial or systematic reproduction, redistribution, reselling, loan, sub-licensing, systematic supply, or distribution in any form to anyone is expressly forbidden. Terms & Conditions of access and use can be found at <http://www.tandfonline.com/page/terms-and-conditions>

Low threshold of distributed feedback lasers based on scaffolding morphologic holographic polymer dispersed liquid crystal gratings: reduced losses through Forster transfer

Lijuan Liu^{a,b}, Wenbin Huang^{a,b}, Zhihui Diao^{a,b}, Zenghui Peng^a, Quan quan Mu^a, Yonggang Liu^a, Chengliang Yang^a, Lifa Hu^a and Li Xuan^{a*}

^aState Key Laboratory of Applied Optics, Changchun Institute of Optics, Fine Mechanics and Physics, Chinese Academy of Sciences, Changchun, Jilin, China; ^bGraduate School of the Chinese Academy of Sciences, Beijing, China

(Received 7 April 2013; accepted 12 September 2013)

The threshold of distributed feedback (DFB) lasing from dye-doped holographic polymer dispersed liquid crystal (HPDLC) gratings was reduced using a guest–host (G–H) system. Different doping concentrations of the guest emitter 4-(dicyanomethylene)-2-methyl-6-(4-dimethylaminostyryl)-4H-pyran (DCM) in the host dye 1,3,5,7,8-pentamethyl-2,6-diethylpyrromethene-difluoroborate (PM567) were dispersed in the HPDLC transmission gratings. DFB lasing was observed in the pure host, the pure guest and in the G–H system. With the increase in doping concentration of the guest, the gain spectrum was redshifted. Through effective Forster energy transfer, we found that the lasing threshold was lowered to 1.35 $\mu\text{J}/\text{pulse}$, which reduced by factor 2 compared to that without energy transfer process. This effect is attributed to the suppression of self-absorption at the lasing wavelength.

Keywords: holographic polymer dispersed liquid crystal; distributed feedback organic laser; Forster energy transfer; low threshold

1. Introduction

Holographic polymer dispersed liquid crystal (HPDLC) gratings have drawn special attention due to a number of applications which include reflective flat panel displays [1], diffraction lenses with switchable focus [2], optical data storage [3], switchable optical phase modulators [4] and optical switches for telecommunications [5]. In this method, two interfering laser beams are used to irradiate a homogeneous syrup, which contains mainly photo-sensitive prepolymer and liquid crystal (LC). In bright regions, the photopolymerisation occurs much more rapidly than in dark regions, resulting in concentration gradients for both monomer and LC. Then, the monomer would diffuse to bright regions to continue the polymerisation and LC molecules would diffuse to dark regions [6]. Finally, a composite system consisting of alternating layers of polymer and LC corresponding to interference fringes is formed. This nanostructure brings in a refractive index modulation at periodicities comparable to the visible wavelength, which enables HPDLC structures to modulate light [7]. Besides, LC molecules can be aligned in the direction of external electric field due to its inherent nature of an anisotropic dielectric, which enables continuous modification of the refractive index in contrast to polymer and LC.

Distributed feedback (DFB) lasers using dye-doped HPDLC structures have attracted much

attention since its first demonstration by Jakubiak [8,9]. The reflection grating was first selected as the laser cavity for obtaining surface-emitting laser emission. Later on, Hsiao et al. reported the laser emission from dye-doped HPDLC transmission grating [10]. Compared with the reflection grating, the transmission grating has a much longer gain length, which facilitates low-threshold laser operation with narrow linewidth. The laser emission intensity from dye-doped HPDLCs can be controlled precisely using a thermal [11] or electrical [10] method. The lasing wavelength also can be tuned thermally [12] or electrically [13,14]. The switching mechanism of the lasers is due to the index modulation of the phase separated LCs. DFB lasers based on HPDLC gratings can also be easily integrated with other optoelectronic elements, since it has a microcavity structure [15]. Besides, the preparation method is very easy with low cost. However, there are still some problems with these lasers, the most important one is high threshold. High threshold will decrease the output lasing energy and limit the operation lifetime of a dye. To decrease the laser threshold, many attempts have been made such as optimising the LC concentration in the prepolymer mixture [11], using two-dimensional (2D) HPDLC square-lattice structures to create stronger coupled electromagnetic bands [16] and using thio-ene monomers to form uniform LC droplets in gratings to decrease scattering loss [17]. The lowest

*Corresponding author. Email: xuanli@ciomp.ac.cn

threshold reported previously was 5 $\mu\text{J}/\text{pulse}$ [11]. The Forster energy transfer from host emitter to guest emitter [18,19] has been demonstrated an effective way to decrease the dye laser threshold and enhance the device performance, since the redshift of the fluorescence spectrum relative to the absorption band of the blend could lower down the losses caused by self-absorption [20]. Recently, low-threshold optically pumped organic lasers using mixtures of organic small molecules have been studied [21–23]. Low thresholds for amplified spontaneous emission [20] and DFB lasers [24] fabricated from blends of conjugated polymers are also reported. However, no threshold behaviour of HPDLC DFB lasers using dye blends as gain medium has been reported.

In this paper, we first demonstrated laser threshold reduction for DFB lasers based on HPDLC transmission gratings through the Forster energy transfer. The emission band was substantially redshifted from the host absorption spectrum with the doping of guest emitter, and absorption loss at the emission wavelengths was decreased. With an optimised doping concentration of the guest dye, the laser threshold is lowered down to 1.35 $\mu\text{J}/\text{pulse}$.

2. Experimental details

2.1 Materials

In our experiments, PM567 and DCM as laser dyes were dissolved directly into the prepolymer mixture, which contained 30 wt.% of acrylate monomer phthalic diglycol diacrylate (PDDA; Sigma-Aldrich), 30 wt.% of acrylate monomer dipentaerythritol hydroxyl pentaacrylate (DPHPA; Sigma-Aldrich), 27.5 wt.% of nematic LC (TEB30A; Slichem), 10 wt.% of N-vinylpyrrolidone (NVP; Sigma-Aldrich) as solvent and chain extender, 1.5 wt.% of co-initiator N-phenylglycine (NPG; Sigma-Aldrich) and 0.5 wt.% of photo-initiator rose Bengal (RB; Sigma-Aldrich). The concentration of PM567 in the mixture was changed from 0.5 wt.% to 0 wt.%, and DCM was changed from 0 wt.% to 0.5 wt.% correspondingly. The wt.% of each

Table 1. wt.% of each dye component used in the prepolymer syrup for samples 1–5.

No.		PM567 (wt.%)	DCM (wt.%)
1	(pure PM567)	0.50	0
2	(2% DCM in PM567)	0.49	0.01
3	(10% DCM in PM567)	0.45	0.05
4	(20% DCM in PM567)	0.40	0.10
5	(pure DCM)	0	0.50

dye component in the syrup is tabulated in Table 1. The chemical structures of PM567 and DCM are shown in Figure 1(a) and (b), respectively. Then, the mixture was stirred for 12 h in the dark until we obtained a homogeneous mixture. The mixture was injected into the empty cells, which were made by two glass plates with a cell gap of 8.5 μm .

2.2 Absorption and fluorescence spectrum measurement

For absorption and fluorescence measurement, each sample was irradiated under a single laser beam from a Nd:YAG laser (532 nm, 10 mW/cm²) for 10 minutes. This homogenous illumination would result in the homogenous dispersion of LC droplets in the polymer matrix which is referred to as polymer dispersed liquid crystal (PDLC). The absorption (Abs) spectra of these composite films were measured using a scanning spectrophotometer (Shimadzu UV-3101; Shimadzu Corp., Kyoto, Japan). The fluorescence spectra were measured by a grating spectrometer (Hitachi F-4500; Hitachi, Ltd., Tokyo, Japan).

2.3 Grating fabrication

Figure 2 shows the schematic set-up for the fabrication of the transmission grating. The cell was irradiated under the interference field formed by two 532 nm Nd:YAG laser beams. By changing the intersection angle 2θ of the two coherent beams, we can get HPDLC transmission gratings with different grating

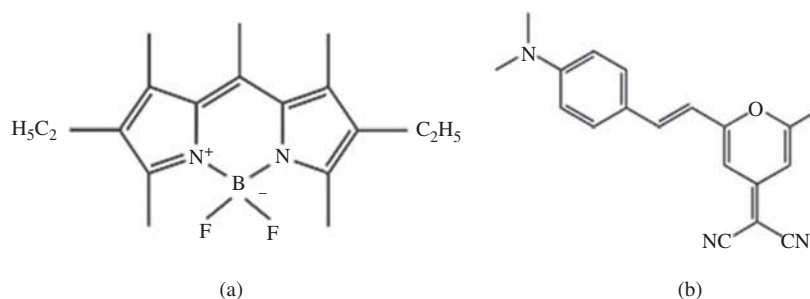


Figure 1. Chemical structures of PM567 (a) and DCM (b).

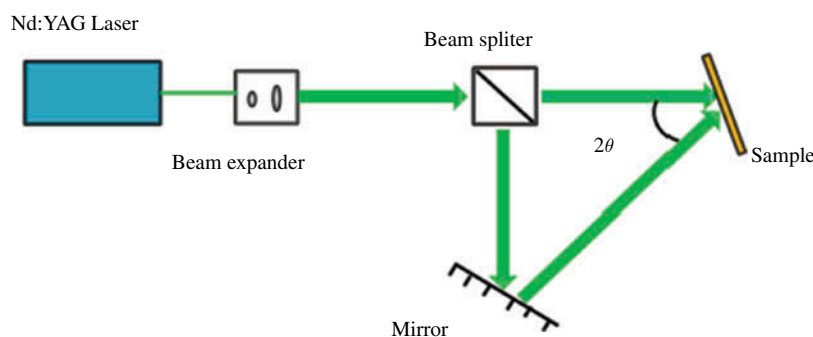


Figure 2. (colour online) Schematic set-up for fabricating the transmission gratings: 2θ – intersection angle.

itches derived by $\Lambda = \frac{\lambda_{532}}{2 \sin \theta}$. The intensity of each recording beam was 10 mW/cm^2 , and the exposure time was about 5 min. Due to the low curing intensity, the resulted grating shows a scaffolding-like morphology, in which the phase-separated LC exists in the form of pure slices instead of droplets and has a fairly good alignment along the grating vector [25]. The grating shows merely scattering, and is very suitable for use as a laser cavity. Specifically, although our gratings share similar peculiar morphology with POLICRYPS (Polymer LIquid CRYstal Polymer Slices) and POLIPHEN (POLYmer LIquid Crystal Polymer Holograms Electrically Manageable), they are realised according to different materials and patented procedures [26]. The recorded grating area was about $8 \text{ mm} \times 8 \text{ mm}$.

2.4 Lasing measurement

The samples were photopumped with a Q-switched frequency-doubled Nd:YAG laser (8 ns, 532 nm, 1 Hz). The schematic set-up for lasing and amplified spontaneous emission (ASE) measurement is shown in Figure 3. The pumping beam was divided by a beam

splitter into two beams with equal intensity. The energy of one beam was detected by a pulse energy meter directly, and the other beam was focused onto the sample to form a narrow stripe ($\sim 0.5 \text{ mm}$) gain area of 10 mm long along the direction perpendicular to the grating layers using a cylindrical lens. Sample (a) in Figure 3 is a HPDLC transmission grating for lasing measurement. The focused stripe can cover thousands of grating periods, and thus ensures sufficient DFB. Sample (b) without grating structure is a PDLC sample for ASE measurement. The reason is that ASE does not require a resonator structure, but a sufficient number of excited states along the optical path [27]. The lasing and ASE output was collected by a fibre pigtail detector, which was coupled to a spectrometer (with a resolution of $\sim 0.25 \text{ nm}$). The output lasing energy was measured by an energy meter (LabMax-TOP; Coherent Inc., Santa Clara, CA, USA).

3. Results and discussions

3.1 Forster energy transfer

The photophysical processes of the energy transfer in the dye blend are shown schematically in Figure 4(a).

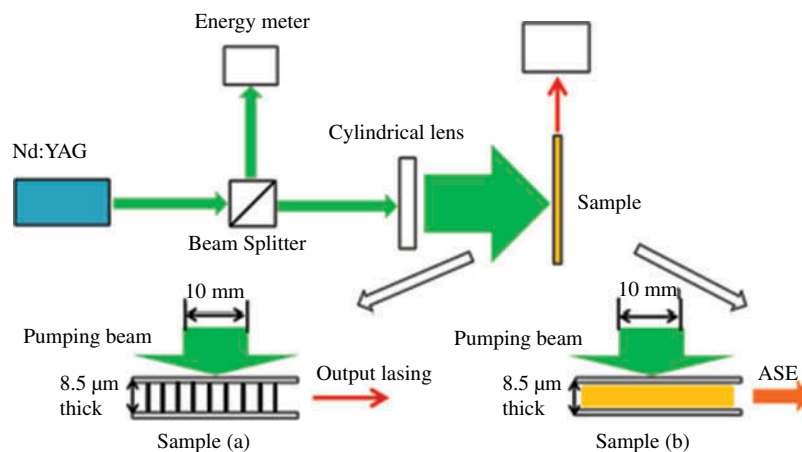


Figure 3. (colour online) Schematic set-up for the lasing (a) and ASE (b) measurement.

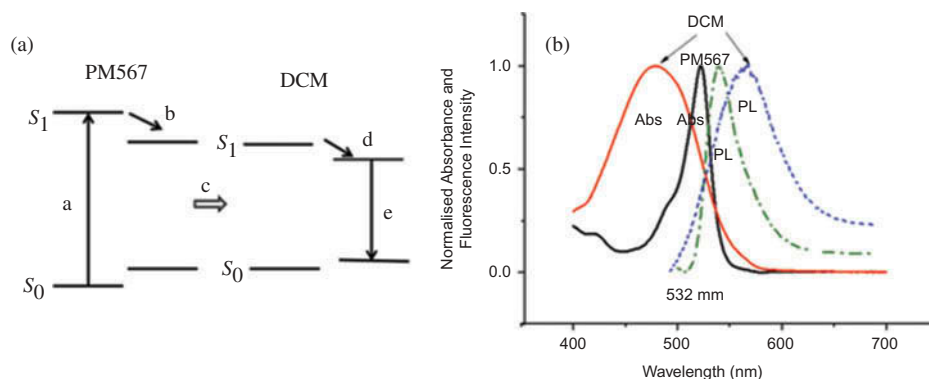


Figure 4. (colour online) (a) Principles of photophysical processes that occur in dye blend. (b) Abs for PM567 (dark solid) and DCM (red solid); PL for PM 567 (green dash) and DCM (blue dash).

PM567 molecules are excited by incident photons from the ground state S_0 to one of the vibrational states of the first singlet manifold S_1 (process a). These molecules relax quickly to the lowest vibrational level in S_1 through an internal relaxation process (process b). The energy of the excited PM567 is then transferred to a nearby DCM molecule (process c) through electromagnetic dipole–dipole interactions. This process known as Forster transfer takes place without the release or absorption of real photons [18]. There is an internal relaxation in the DCM molecule (process d) as well, and it is followed by real photons emission (process e). Forster energy transfer from the host dye PM567 to the guest dye DCM can lead to lower self-absorption losses as the emission is redshifted [18,20]. The rate of Forster transfer K_{GH} follows the equations [18,28,29]:

$$K_{HG} = \frac{1}{\tau_H} \frac{1}{R^6} \left(\frac{3}{4\pi} \int \frac{C^4}{\omega^4 n^4} F_H(\omega) \sigma_D(\omega) d\omega \right) \quad (1)$$

where τ_H is the natural radiative lifetime of the host, R is the mean host–guest spacing, $F_H(\omega)$ and $\sigma_D(\omega)$ is the normalised spectral distribution of host emission and guest absorption as a function of frequency ω , respectively. From these equations, we can conclude that a larger spectral overlap between the emission of the host and the absorption of the guest could lead to a higher rate of Forster transfer. Small G–H spacing (typically between 1 and 10 nm) [18] is necessary for strong dipole–dipole interactions, which is also a very important factor for transfer process [30]. In Figure 4(b), the Abs and the PL spectra of both host dye and guest dye are shown. In the spectral range of 510–570 nm there is an obvious overlap between Abs spectra of PM567 and PL spectra of DCM, thereby efficient Forster type energy transfer can be anticipated in our dye blend. Besides, a large host–guest spacing slows down the rate of excitation transfer,

so increasing the guest concentration is necessary for effective energy transfer.

3.2 Absorption spectrum and ASE spectrum

Figure 5 shows absorption spectrum for PM567, DCM and their blends. The absorption spectrum of their blends are similar to the absorption spectrum of pure PM567, indicating that absorption originates from the host dye. ASE is a useful tool to explore effective lasing conditions [27,31], such as the output lasing wavelength region and the threshold distribution at different wavelengths. ASE narrows the emission spectrum because the amplification is maximum at the wavelength where the net gain is highest [30]. In the blend dyes, some excitations of the host dye may decay radiatively, while other excitations are deactivated through the Forster energy transfer with the guest dye. Once the energy is transferred to the guest emitters, emission is observed from the guest molecules as well.

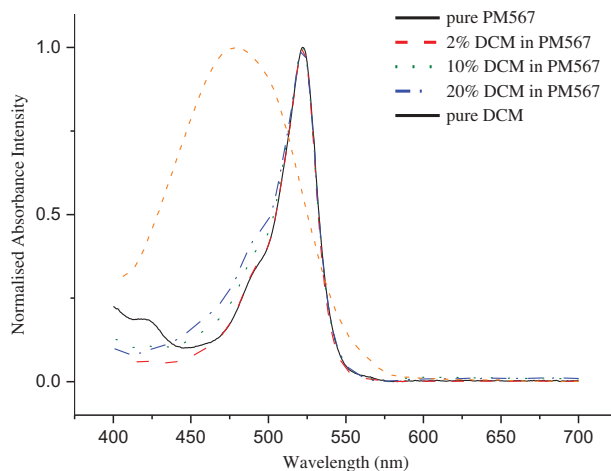


Figure 5. (colour online) Absorption spectrum for PM567, DCM and their blends.

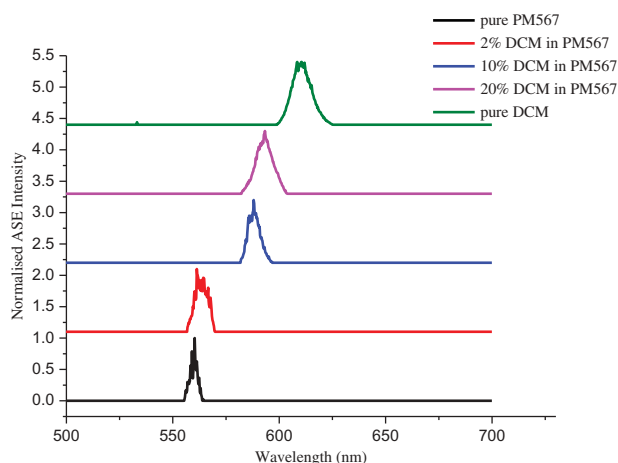


Figure 6. (colour online) ASE (amplified spontaneous emission) for PM567, DCM and their blends.

From Figure 6, we can see the ASE peak barely redshifts compared with pure PM567, though the sample with a guest doping concentration of 2% in PM567. It indicated that the doping concentration was too small for efficient energy transfer to occur due to the large host–guest spacing. By increasing the DCM doping concentration to 10% in PM567, the average host–guest spacing decreases, and the rate of energy transfer increases. Energy transfer takes place before a significant fraction of the excitations in the host polymer decay radiatively, thus the emission from the guest molecules eventually dominates the emission spectrum. The ASE peak moves to 588 nm compared with 560 nm in pure host. Further increasing the guest concentration would further redshift the gain spectrum, but to a less extent. Thus, the overlap of PL spectra and Abs spectra of the blend decreases as a result of the redshift of PL spectra, thereby the re-absorption loss is reduced.

3.3 lasing threshold performance

DFB lasing relies on the positive feedback distributed in the periodic structure. The output lasing wavelength λ_0 can be calculated using the Bragg's equation:

$$\frac{\lambda_0}{m} = 2n_{eff} \Lambda \quad (2)$$

where n_{eff} is the effective refractive index, Λ is the grating pitch, and m is the Bragg order which is selected as 3 in this work. Thus, we can obtain lasing output throughout the gain spectrum of each blend by varying the grating periodicity.

We obtained lasing output from 550 nm to 603 nm for pure PM567, from 568 nm to 618 nm for 2% DCM in PM567, from 568 nm to 638 nm for 10% DCM in

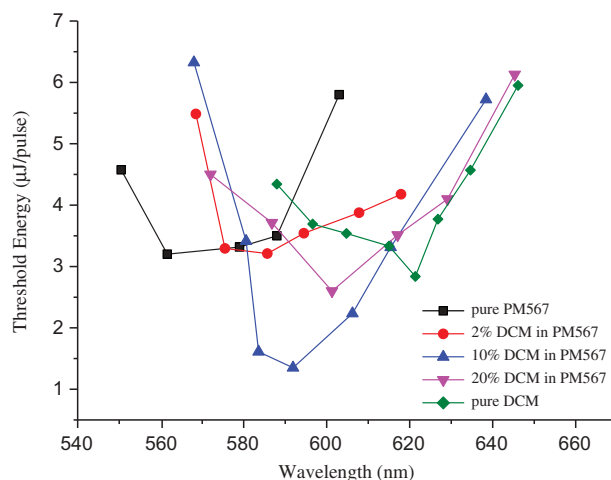


Figure 7. (colour online) Dependence of threshold energy on the lasing wavelength for pure PM567 (square), 2% DCM in PM567 (sphere), 10% DCM in PM567 (top triangle), 20% DCM in PM567 (bottom triangle) and pure DCM (diamond), respectively.

PM567, from 572 nm to 645 nm for 20% DCM in PM567 and from 584 nm to 654 nm for pure DCM. The periods of the gratings are from 532 nm to 596 nm, from 549 nm to 607 nm, from 549 nm to 618 nm, from 567 nm to 618 nm and from 567 nm to 641 nm, correspondingly. The lasing threshold as a function of output wavelength is shown in Figure 7. The lowest threshold obtained for each dye system is at its corresponding ASE maximum where the net gain is the highest. The wavelength at the lowest threshold for each mixture is redshifted with increasing concentration of guest dye DCM. Figure 8 shows lowest lasing threshold energy for each dye blend. The blend of 2% DCM in PM567 has little redshift, and the energy

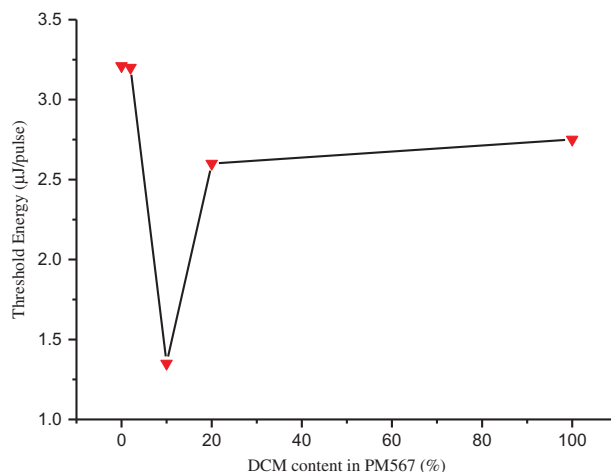


Figure 8. (colour online) Lowest laser threshold for each group.

transfer from PM567 to DCM is incomplete. Its lowest threshold is almost the same as pure PM567, since the self-absorption is not substantially decreased. At a high guest doping concentration of 20% in PM567, the lowest threshold 2.6 $\mu\text{J}/\text{pulse}$ is still high due to the decrease in host absorption efficiency at the pumping wavelength. The DCM doping concentration of 10% in PM567 is found to be the best trade-off between low self-absorption and high host absorption efficiency. The lowest threshold energy in this doped system was measured to be 1.35 $\mu\text{J}/\text{pulse}$ at 591.9 nm.

This indicates a threshold reduction by a factor 2 compared to 2.75 $\mu\text{J}/\text{pulse}$ for pure guest and even by a factor 3 in relation the 3.21 $\mu\text{J}/\text{pulse}$ for pure host.

Figure 9(a) shows the output lasing energy as a function of pump intensity for the DFB laser fabricated with pure PM567. It was observed that the light intensity increased linearly above the threshold of 3.21 $\mu\text{J}/\text{pulse}$ with increasing pump energy, and the lasing slope efficiency of this HPDLC grating with dye blends is about 0.3%. The inset shows the corresponding lasing spectra. The lasing peak is 561.7 nm, and its full

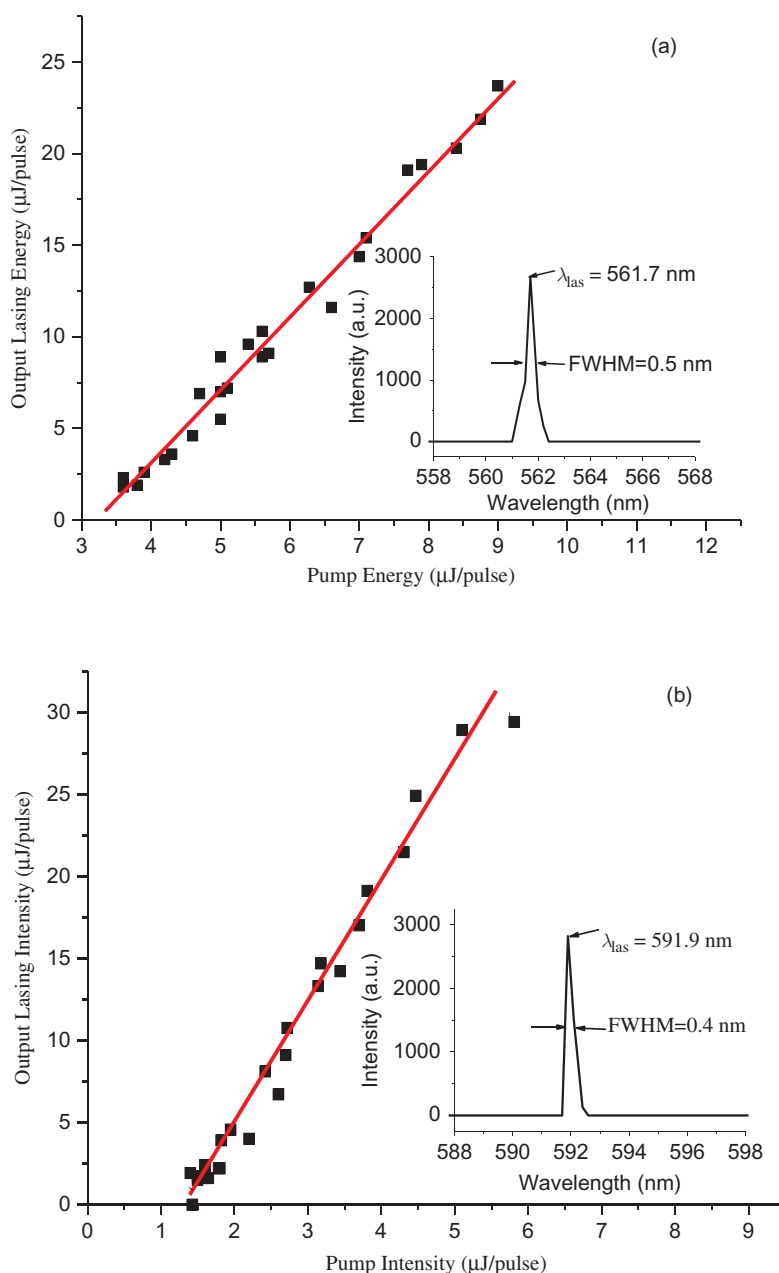


Figure 9. (colour online) Output lasing intensity as a function of pump intensity for the DFB laser fabricated: (a) with 10% DCM in PM567, (b) with pure PM567. The insets show the corresponding lasing spectra, respectively.

width at half maximum (FWHM) is around 0.5 nm. The output lasing energy as a function of pump intensity for the DFB laser fabricated with 10% DCM in PM567 is shown in Figure 9(b). Compared to the pure-guest system, the threshold is decreased to 1.35 $\mu\text{J}/\text{pulse}$ and the lasing slope efficiency is improved to 0.7% at the same time. The inset shows the corresponding lasing spectra. The lasing peak is 591.9 nm, and its FWHM is only 0.4 nm. Through efficient Forster type energy transfer, the properties of the lasers have been improved.

4. Conclusion

In summary, we first report the lowering of lasing threshold in two dyes blend by forster energy transfer from host dye PM567 to guest dye DCM based on HPDLC gratings. At a DCM doping concentration of 10% in PM567, the lowest threshold energy was found to be 1.35 $\mu\text{J}/\text{pulse}$, which is less than half of that without energy transfer processes. Besides, the energy conversion is much improved. The energy transfer process provides an efficient method to lower lasing threshold particularly for dyes with a small Stokes shift.

Acknowledgements

The authors thank the Natural Science Foundation of China (grant Nos [11174274], [11174279], [61205021], [11204299], [61378075], [61377032]) for their support.

References

- [1] Date M, Takeuchi Y, Kato K. A memory-type holographic polymer dispersed liquid crystal (HPDLC) reflective display device. *J Phys D: Appl Phys*. 1998;31:2225–2230.
- [2] Hsiao VKS, Chang W-T. Optically switchable, polarization-independent holographic polymer dispersed liquid crystal (H-PDLC) gratings. *Appl Phys B*. 2010;100:539–546.
- [3] Simoni F, Cipparrone G, Mazzulla A, Pagliusi P. Polymer dispersed liquid crystals: effects of photorefractivity and local heating on holographic recording. *Chem Phys*. 1999;245:429–436.
- [4] Sio LD, Tabiryan N, Caputo R, Veltri A, Umeton C. POLICRYPS structures as switchable optical phase modulators. *Opt Express*. 2008;16:7619–7624.
- [5] Li MS, Wu ST, Fuh AY-G. Superprism phenomenon based on holographic polymer dispersed liquid crystal films. *Appl Phys Lett*. 2006;88:091109.
- [6] Lucchetta DE, Criante L, Francescangeli O, Simoni F. Light amplification by dye-doped holographic polymer dispersed liquid crystals. *Appl Phys Lett*. 2004;84:4893–4895.
- [7] Yablonovitch E. Inhibited spontaneous emission in solid-state physics and electronics. *Phys Rev Lett*. 1987;58:2059–2062.
- [8] Jakubiak R, Bunning TJ, Vaia RA, Natarajan LV, Tondiglia PV. Electrically switchable, one-dimensional polymeric resonators from holographic photopolymerization: a new approach for active photonic bandgap materials. *Adv Mater*. 2003;15:241–244.
- [9] Jakubiak R, Natarajan LV, Tondiglia V, He GS, Prasad PN, Bunning TJ, Vaia RA. Electrically switchable lasing from pyrromethene 597 embedded holographic-polymer dispersed liquid crystals. *Appl Phys Lett*. 2004;85:6095–6097.
- [10] Hsiao VKS, Lu C, He GS, Pan M, Cartwright AN, Prasad PN. High contrast switching of distributed-feedback lasing in dye-doped H-PDLC transmission grating structures. *Opt Express*. 2005;13:3787–3794.
- [11] Liu YJ, Sun XW, Elim HI, Ji W. Effect of liquid crystal concentration on the lasing properties of dye-doped holographic polymer-dispersed liquid crystal transmission gratings. *Appl Phys Lett*. 2007;90:011109.
- [12] Deng S, Huang W, Liu Y, Diao Z, Peng Z, Yao L, Xuan L. Wavelength tunable properties for distributed feedback lasing from dye-doped holographic polymer dispersed liquid crystal transmission grating. *Acta Phys Sin*. 2012;61:126101.
- [13] Huang W, Diao Z, Yao L, Cao Z, Liu Y, Ma J, Xuan L. Electrically tunable distributed feedback laser emission from scaffolding morphologic holographic polymer dispersed liquid crystal grating. *Appl Phys Express*. 2013;6:022702.
- [14] Lucchetta DE, Criante L, Francescangeli O, Simoni F. Wavelength flipping in laser emission driven by a switchable holographic grating. *Appl Phys Lett*. 2004;84:837–839.
- [15] Ye C, Shi L, Wang J, Lo D, Zhu X-G. Simultaneous generation of multiple pairs of transverse electric and transverse magnetic output modes from titania zirconia organically modified silicate distributed feedback waveguide lasers. *Appl Phys Lett*. 2003;83:4101–4103.
- [16] Jakubiak R, Tondiglia VP, Natarajan LV, Sutherland RL, Lloyd P, Bunning TJ, Vaia RA. Dynamic lasing from all-organic two-dimensional photonic crystals. *Adv Mater*. 2005;17:2807–2811.
- [17] Jakubiak R, Brown DP, Natarajan LV, Tondiglia V, Lloyd P, Sutherland RL, Bunning TJ, Vaia RA. Influence of morphology on the lasing behavior of pyrromethene 597 in a holographic polymer dispersed liquid crystal reflection grating. *Proc SPIE*. 2006;6322:63220A.
- [18] Förster T. 10th Spiers memorial lecture transfer mechanisms of electronic excitation. *Discuss Faraday Soc*. 1959;27:7–17.
- [19] May B, Poteau X, Yuan D, Brown RG. A study of a highly efficient resonance energy transfer between 7-*N,N*-diethylamino-4-methylcoumarin and 9-butyl-4-butylamino-1,8-naphthalimide. *Dyes Pigments*. 1999;42:79–84.
- [20] Gupta R, Stevenson M, Dogariu A, McGehee MD, Park JY, Srdanov V, Heeger AJ. Low-threshold amplified spontaneous emission in blends of conjugated polymers. *Appl Phys Lett*. 1998;73:3492–3494.
- [21] Berggren M, Dodabalapur A, Slusher RE. Stimulated emission and lasing in dye-doped organic thin films with Forster transfer. *Appl Phys Lett*. 1997;71:2230–2232.
- [22] Kozlov VG, Bulovic V, Burrows PE, Baldo M, Khalfin VB, Parthasarathy G, Forrest SR. Study of lasing

- action based on Förster energy transfer in optically pumped organic semiconductor thin films. *J Appl Phys.* 1998;84:4096–4107.
- [23] Berggren M, Dodabalapur A, Slusher RE, Bao Z. Light amplification in organic thin films using cascade energy transfer. *Nature.* 1997;389:466–469.
- [24] Gupta R, Stevenson M, Heeger AJ. Low threshold distributed feedback lasers fabricated from blends of conjugated polymers: reduced losses through Förster transfer. *J Appl Phys.* 2002;92:4874–4877.
- [25] Huang W, Liu Y, Diao Z, Yang C, Yao L, Ma J, Xuan L. Theory and characteristics of holographic polymer dispersed liquid crystal transmission grating with scaffolding morphology. *Appl Opt.* 2012;51:4013–4020.
- [26] Abbate G, Vita F, Marino A, Tkachenko V, Slussarenko S, Sakhno O, Stumpe J. New generation of holographic gratings based on polymer-LC composites: POLICRYPS and POLIPHEN. *Mol Cryst Liq Cryst.* 2006;453:1–13.
- [27] Kretsch KP, Belton C, Lipson S, Blau WJ, Henari FZ. Amplified spontaneous emission and optical gain spectra from stilbenoid and phenylene vinylene derivative model compounds. *J Appl Phys.* 1999;86: 6155–6159.
- [28] Förster T. *Modern quantum chemistry: action of light and organic molecules.* New York (NY): Academic Press; 1965.
- [29] Pope M, Swenberg CE. *Electronic processes in organic crystals.* New York (NY): Oxford University Press; 1982.
- [30] McGehee MD, Gupta R, Veenstra S, Miller EK, Diaz-Garcia M, Heeger AJ. Amplified spontaneous emission from photopumped films of a conjugated polymer. *Phys Rev B.* 1998;58:7035–7039.
- [31] Tsutsumi N, Kawahira T, Sakai W. Amplified spontaneous emission and distributed feedback lasing from a conjugated compound in various polymer matrices. *Appl Phys Lett.* 2003;83:2533–2535.